Fractals, Vol. 5, No. 4 (1997) 603–614

FRACTAL TREES WITH SIDE BRANCHING

W. I. NEWMAN
Departments of Earth and Space Sciences,
Physics and Astronomy, and Mathematics
University of California, Los Angeles, CA 90095

D. L. TURCOTTE
Department of Geological Sciences
Cornell University, Ithaca, NY 14853

A. M. GABRIELOV
Departments of Mathematics, and Earth
and Atmospheric Sciences
Purdue University, West Lafayette, IN 47907

Received Apirl 16, 1997; Accepted May 15, 1997

Abstract

This paper considers fractal trees with self-similar side branching. The Tokunaga classification system for side branching is introduced, along with the Tokunaga self-similarity condition. Area filling ($D = 2$) and volume filling ($D = 3$) deterministic fractal tree constructions are introduced both with and without side branching. Applications to diffusion limited aggregation (DLA), actual drainage networks, as well as biology are considered. It is suggested that the Tokunaga taxonomy may have wide applicability in nature.

1. INTRODUCTION

Fractal trees have been employed in a wide variety of applications including drainage networks, actual plants and trees, root systems, bronchial systems, cardiovascular systems, and evolution. Prior to the introduction of fractals by Mandelbrot,[1] empirical studies of drainage networks[2] had given power-law relations between stream numbers, stream lengths, drainage areas, and stream slopes.

The original branch ordering taxonomy for fractal trees was developed as a stream-ordering system in geomorphology by Horton[2] and Strahler[3]. Streams on a standard topographic map with no upstream tributaries are defined to be first order ($i = 1$). When two first-order streams combine they form a second-order ($i = 2$) stream. When two second-order streams combine, they form a third-order ($i = 3$) stream, and so forth. Horton[2] also

introduced the bifurcation ratio

$$R_b = \frac{N_i}{N_{i+1}} \tag{1}$$

and the length-order ratio

$$R_r = \frac{r_{i+1}}{r_i} \tag{2}$$

where N_i is the number of streams of order i, and r_i is the mean length of streams of order i. Empirically it was found that R_b and R_r were nearly constant, independent of order, for actual drainage networks.

With the introduction of the fractal dimension D as the power-law scaling exponent between number and length, it was recognized that the fractal dimension of a stream network is given by

$$D = \frac{\ln R_b}{\ln R_r}\,. \tag{3}$$

Typical drainage networks have fractal dimensions near 1.8.

A small example of a typical drainage network is given in Fig. 1(a). The 100 m scale is shown, without the specified scale it would be impossible to tell whether the drainage network covered 1 km or 1000 km. An example of a binary deterministic fractal tree is given in Fig. 1(b). This is a highly ordered structure in which the single stem bifurcates into two branches, each with one-half the length of the stem, these two branches in turn bifurcate to form four branches each with one-quarter the length of the stem. Obviously this construction could be carried to higher and higher orders. The stream-ordering system is illustrated for this tree which has $R_b = 2$, $R_r = 2$, and $D = 1$.

However, there is a major difference between the binary fractal tree illustration in Fig. 1(b) and the drainage network illustrated in Fig. 1(a). Drainage networks have side-branching; that is, some first-order streams intersect second-order, third-order, and all higher-order streams. Similarly, second-order streams intersect third-order and higher-order streams, and so forth. To classify side branching Tokunaga[4–6] extended the Strahler[3] ordering system. A first-order branch intersecting a first-order branch is denoted "11" and the number of such branches is N_{11}, a first-order branch intersecting a second-order branch is denoted "12" and the number of such branches is N_{12}, a second-order branch intersecting a second-order branch is denoted "22" and the number of such branches is N_{22} and so forth. The total number of streams of order i, N_i, is related to the N_{ij} by

$$N_i = \sum_{j=1}^{n} N_{ij} \tag{4}$$

for a fractal tree of order n. A deterministic fractal tree with side branching is illustrated in Fig. 1(c). This fractal construction has $R_r = 2$ but R_b is not constant. However, it is easy to show that $R_b \to 4$ for large i. Thus from Eq. (3) $D \to 2$ for large i.

The branch numbers N_{ij}, $i < j$, constitute a square upper-triangular matrix. This formulation is illustrated in Fig. 2(a), the branch-number matrices for the drainage network and deterministic fractals illustrated in Fig. 1(a)–(c) are given in Fig. 2(b)–(d). This class of fractal trees can also be quantified in terms of branching ratios T_{ij}, these are the average number of branches of order i joining branches of order j. Branching ratios are related to branch

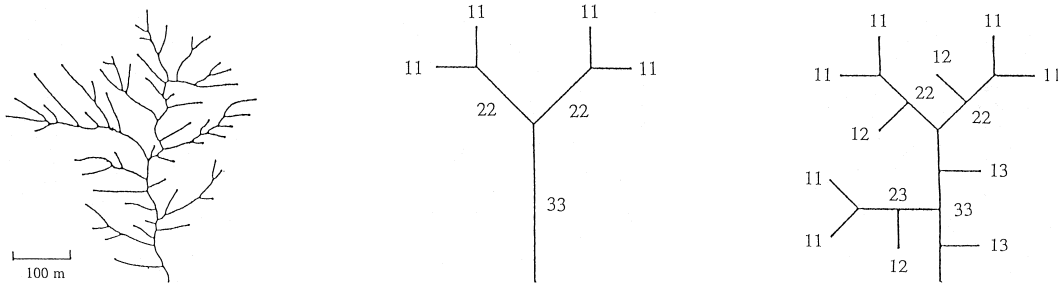

(a) (b) (c)

Fig. 1 **(a)** Example of a fourth-order drainage network. **(b)** Binary self-similar fractal tree. **(c)** Binary self-similar fractal tree with side branches.

$$\begin{array}{cccc} N_{11} & N_{12} & N_{13} & N_{14} \\ & N_{22} & N_{23} & N_{24} \\ & & N_{33} & N_{34} \\ & & & N_{44} \end{array} \qquad \begin{array}{c} N_1 \\ N_2 \\ N_3 \\ N_4 \end{array} \qquad \begin{array}{cccc} 20 & 26 & 8 & 7 \\ & 4 & 3 & 3 \\ & & 2 & 0 \\ & & & 1 \end{array} \qquad \begin{array}{c} 51 \\ 10 \\ 2 \\ 1 \end{array} \qquad \begin{array}{ccc} 4 & 0 & 0 \\ & 2 & 0 \\ & & 1 \end{array} \qquad \begin{array}{c} 4 \\ 2 \\ 1 \end{array} \qquad \begin{array}{ccc} 6 & 3 & 2 \\ & 2 & 1 \\ & & 1 \end{array} \qquad \begin{array}{c} 11 \\ 3 \\ 1 \end{array}$$

(a) (b) (c) (d)

Fig. 2 **(a)** Illustration of the branch-number matrix. **(b)–(d)** Branch number matrices for the fractal trees illustrated in Fig. 1 (a)–(c).

$$\begin{array}{ccc} T_{12} & T_{13} & T_{14} \\ & T_{23} & T_{24} \\ & & T_{34} \end{array} \qquad \begin{array}{ccc} 2 & 4 & 7 \\ & 1.5 & 3 \\ & & 0 \end{array} \qquad \begin{array}{ccc} 0 & 0 \\ & 0 \end{array} \qquad \begin{array}{cc} 1 & 2 \\ & 1 \end{array}$$

(a) (b) (c) (d)

Fig. 3 **(a)** Illustration of the branching-ratio matrix. **(b)–(d)** Branching-ratio matrices for the fractal trees illustrated in Fig. 1 (a)–(c).

numbers by

$$T_{ij} = \frac{N_{ij}}{N_j} \,. \tag{5}$$

Again the branching ratios T_{ij} constitute a square, upper-triangular matrix as illustrated in Fig. 3(a). The branching ratio matrices for the drainage network and deterministic fractals illustrated in Fig. 1(a)–(c) are given in Fig. 3(b)–(d).

We now define self-similar trees to be the subset of trees for which $T_{i,i+k} = T_k$ where T_k is a branching ratio that depends on k but not on i. Tokunaga[4–6] introduced a more restricted class of self-similar, side-branching trees by requiring for self-similarity of side branching that

$$T_k = a\, c^{k-1} \,. \tag{6}$$

This is now a two parameter family of trees and we will define fractal trees in this class to be Tokunaga trees. For the fractal tree illustrated in Fig. 1(c) we have $a = 1$ and $c = 2$.

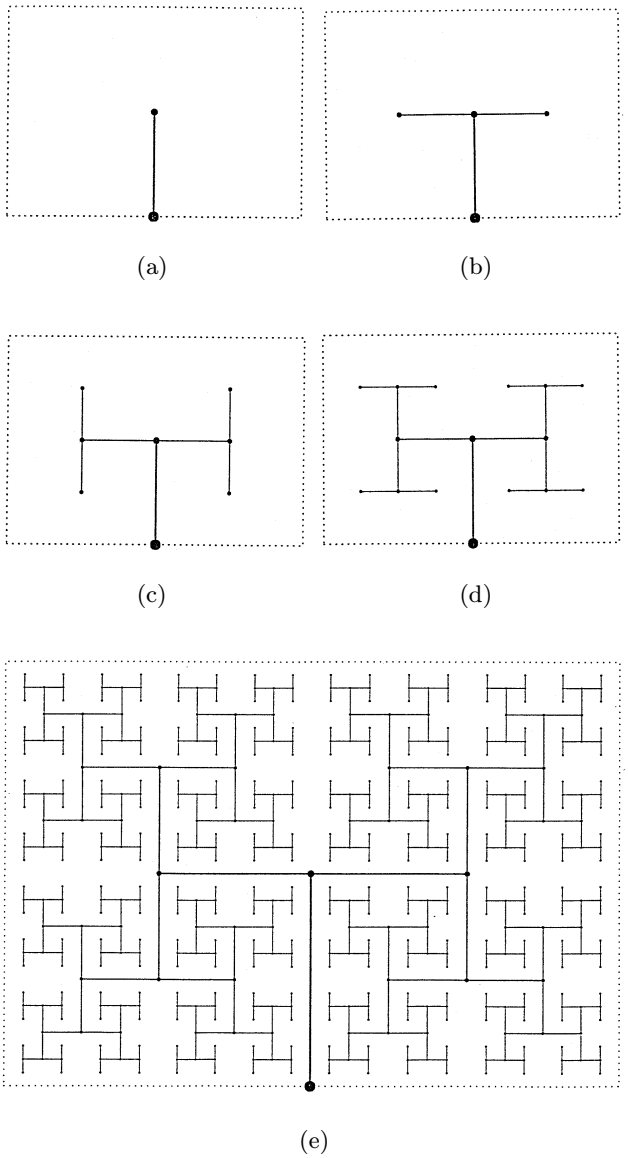

Fig. 4 Deterministic binary fractal tree. With $R_b = 2$ and $R_r = 2^{1/2}$ we have $D = 2$, the construction is area filling without overlap. **(a)** First-order example. **(b)** Second-order example. **(c)** Third-order example. **(d)** Fourth-order example. **(e)** Ninth-order example.

2. AREA AND VOLUME FILLING FRACTAL TREES

We will now consider a sequence of deterministic fractal trees that are either area filling ($D = 2$) or volume filling ($D = 3$). We will consider trees with and without side branching and will begin with examples of area filling trees. A deterministic space-filling fractal tree without side branching is illustrated in Fig. 4. For this binary tree we have $R_b = 2$ and $R_r = 2^{1/2}$ so that $D = 2$. When carried to infinite order this fractal tree fills the rectangular region of unit height and width $2^{1/2}$ without overlap.

The generator for this construction is the branch with length 1/2 that extends at first order from the center of the boundary to the center of the rectangular region [Fig. 4(a)]. There is a tip node at the end of this branch. The rectangular region is then divided into two equal parts and the construction is extended to second order. Two tip branches with lengths $1/2^{3/2}$ emanate from the first-order node [Fig. 4(b)]. There are two second-order tip nodes at the ends of these branches. This construction can be extended to arbitrarily high order.

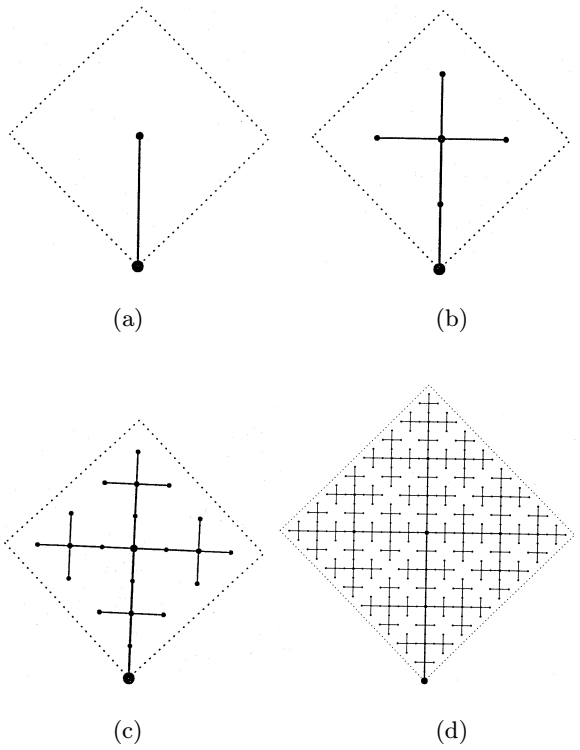

Fig. 5 Deterministic ternary fractal tree with side branching based on a square. With $R_r = 2$ this construction is area filling. **(a)** Third-order example. **(b)** Fifth-order example.

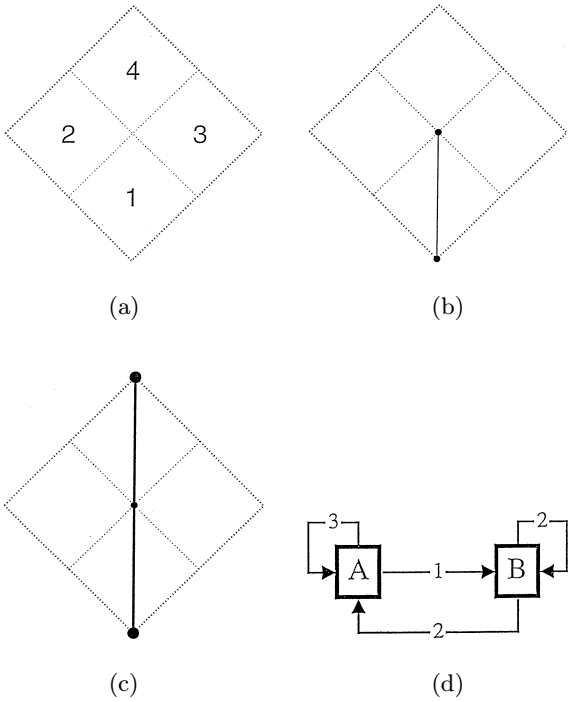

Fig. 6 **(a)** At each order the square is divided into four equal sized squares, the numbering of the squares is given. **(b)** Generator A required in the construction illustrated in Fig. 5. **(c)** Generator B required in the construction illustrated in Fig. 5(d). **(d)** Flow chart indicating how the generators A and B in Fig. 6 are used to construct the fractal tree illustrated in Fig. 5.

A deterministic area-filling fractal tree with side branching is illustrated in Fig. 5. The first three iterations, and the fifth-order example of this ternary tree are given. In order to construct this fractal tree we use a generator A given in Fig. 6(b). The first-order branch extends from a corner of the unit square to its center and there is a tip node at its end. The unit square is then divided into four equal squares with $r = 1/2$. These four squares are numbered 1 to 4 as shown in Fig. 6(a). As the second-order branches, we use the scaled generator A, extending it from the tip of the first-order branch to the centers of the four squares, and place tip nodes at the end of each new branch. Squares 2, 3, and 4 are now scaled versions of the original square. However, in square 1 we have overlapping with the previously drawn tree, and an internal second-order node appears at the center of the first-order branch. Geometrically, it is the same as using a second generator B [Fig. 6(c)]. Each of the four squares at second order is further divided to give four squares with $r_3 = 1/4$ at third order. Each of the squares 2, 3, and 4 produces three squares with generator A and one square with generator B, while square 1 produces two squares with generator A and two squares with generator B. At third order there are nine tip branches, two side branches, eleven tip nodes, and five internal nodes. These steps are repeated at all higher orders. A flow chart illustrating the construction of this fractal tree is given in Fig. 6(d).

The length-order ratio for this construction is $R_r = 2$. The branch-number and branch-ratio matrices for this construction are given in Fig. 7(a) and 7(c). The branching ratios for arbitrary order are given by

$$T_k = \begin{cases} 0, & \text{k=1} \\ 2^{k-1}, & \text{k= } 2, 3, \ldots \end{cases} . \tag{7}$$

The construction is a Tokunaga fractal tree. The branch numbers and bifurcation ratios are given in Fig. 8(b). For large-order trees R_b becomes independent of order and $R_b \to 4$; thus $D \to 2$ and the construction becomes space filling.

The number of squares requiring generator A at order i is $n_A(i)$ and the number of squares requiring generator B at order i is $n_B(i)$. From the flow

$N_{11} = 129$	$N_{12} = 0$	$N_{13} = 22$	$N_{14} = 12$	$N_{15} = 8$
	$N_{22} = 33$	$N_{23} = 0$	$N_{24} = 6$	$N_{25} = 4$
		$N_{33} = 9$	$N_{34} = 0$	$N_{35} = 2$
			$N_{44} = 3$	$N_{45} = 0$
				$N_{55} = 1$

(a)

$N_1 = 171$	$R_{b12} = 3.98$	$T_{12} = 0$	$T_{13} = 2$	$T_{14} = 4$	$T_{15} = 8$
$N_2 = 43$	$R_{b23} = 3.91$		$T_{23} = 0$	$T_{24} = 2$	$T_{25} = 4$
$N_3 = 11$	$R_{b34} = 3.67$			$T_{34} = 0$	$T_{35} = 2$
$N_4 = 3$	$R_{b45} = 3.00$				$T_{45} = 0$
$N_5 = 1$					

(b) (c)

Fig. 7 **(a)** Branch number matrix for the Tokunaga tree illustrated in Fig. 5. **(b)** Branch numbers and bifurcation ratios. The bifurcation ratio approaches 4 ($D \to 2$) for high orders. **(c)** Branch-ratio matrix for the tree.

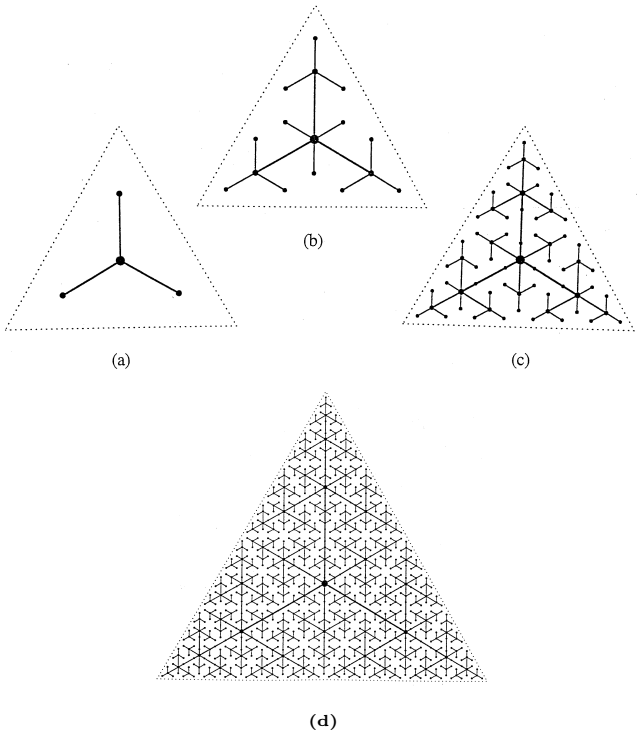

Fig. 8 Deterministic ternary fractal tree with side branching based on an equilateral triangle. With $R_r = 2$ the construction is area filling without overlap. **(a)** First-order example. **(b)** Second-order example. **(c)** Third-order example. **(d)** Fifth-order example.

chart, Fig. 6(d), we have the recursive map

$$n_A(i+1) = 3n_a(i) + 2n_b(i) \tag{8}$$

$$n_b(i+1) = n_A(i) + 2n_B(i)\,. \tag{9}$$

Defining the vector

$$\vec{n}_i = \begin{pmatrix} n_A(i) \\ n_B(i) \end{pmatrix} \tag{10}$$

we can write

$$\vec{n}_{i+1} = A\vec{n}_i \tag{11}$$

where the matrix A is given by

$$A = \begin{pmatrix} 3 & 2 \\ 1 & 2 \end{pmatrix}\,. \tag{12}$$

The eigenvalues of this matrix are $\lambda = 4, 1$. For large orders the eigenvalue $\lambda = 4$ dominates and this is consistent with $R_b \to 4$.

The space filling construction considered above is far from unique. An alternative deterministic ternary fractal tree that is space filling is illustrated in Fig. 8. This construction is based on equilateral triangles. In order to construct this fractal tree we require the six generators given in Fig. 9(b)–(g). At first order we begin with generator O [Fig. 9(b)] and divide the unit equilateral triangle into four equilateral triangles with $r_2 = 1/2$. These four equilateral triangles are numbered 1 to 4 as shown in Fig. 9(a). Generator 0 will not be used in further iterations. In triangles 1, 2, and 3 we use generator A [Fig. 9(c)] at second order and in square 4 we use generator P [Fig. 9(d)] at second order. Generator P will also not be used in further iterations. Each of the four triangles at second order is further divided into four triangles with $r_3 = 1/4$ at third order. The triangles generated using A require the use of generator A in triangles 1, 2, and 3 and generator B [Fig. 9(e)] in triangle 4. The triangle generated using P requires the use of generator A in triangles 1, 2, and 3 and generator C [Fig. 9(f)] in triangle 4. At the next iteration it is necessary to specify the treatment of the generators B and C. Considering generator B we use generator A in triangles 1 and 2, generator D [Fig. 9(g)] in triangle 3, and generator C in triangle 4. Considering generator C, we use generator D in triangles 1, 2, and 3 and generator C in triangle 4. At the next iteration it is necessary to specify the treatment of generator D, we use generator A in triangles 1 and 2, generator D in triangle 3, and generator B in triangle 4. These steps are repeated at all higher orders. A flow chart illustrating the construction of the fractal tree is given in Fig. 9(h).

The length-order ratio for this construction is $R_r = 2$. The branch-number and branch-ratio matrices for this construction are given in Fig. 10(a) and 10(c). Except for one initial branching this construction is also a Tokunaga fractal tree that satisfies Eq. (7). The branch number and bifurcation

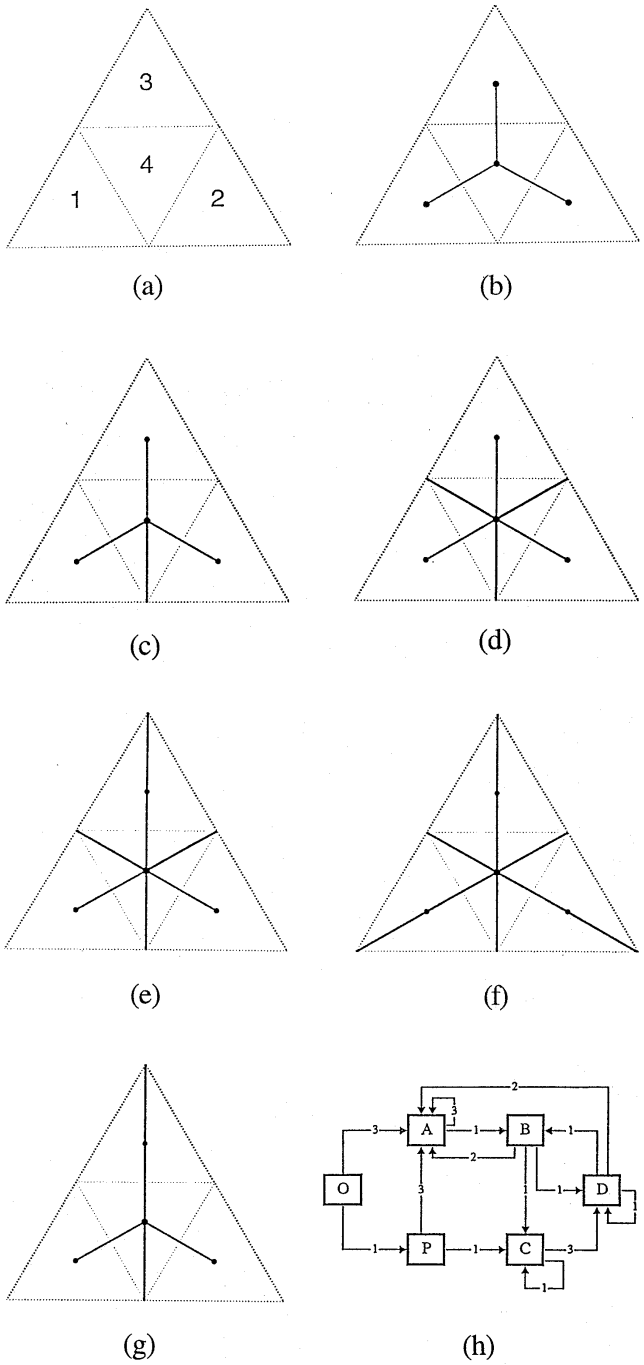

Fig. 9 **(a)** At each order the equilateral triangle is divided into four equal sized equilateral triangles, the numbering of the triangles is given. **(b)–(g)** The six generators required to carry out the construction illustrated in Fig. 8. **(h)** Flow chart indicating how the generators O, P, A, B, C, and D are used to construct the fractal tree illustrated in Fig. 8.

ratios are given in Fig. 10(b). Again $R_b \to 4$ and $D \to 2$ for large orders and the construction is space filling.

The recursive map for this construction is

$$n_A(i+1) = 3n_A(i) + 2n_B(i) + 2n_D(i) \quad (13)$$

$$n_B(i+1) = n_A(i) + n_D(i) \quad (14)$$

$$n_C(i+1) = n_B(i) + n_C(i) \quad (15)$$

$$n_D(i+1) = n_B(i) + 3n_C(i) + n_D(i)\,. \quad (16)$$

$N_{11} = 486$ $N_{12} = 0$ $N_{13} = 84$ $N_{14} = 48$ $N_{15} = 24$
$N_{22} = 126$ $N_{23} = 0$ $N_{24} = 24$ $N_{25} = 12$
$N_{33} = 36$ $N_{34} = 0$ $N_{35} = 6$
$N_{44} = 9$ $N_{45} = 0$
$N_{55} = 3$

(a)

$N_1 = 642$
$N_2 = 162$
$N_3 = 42$
$N_4 = 12$
$N_5 = 3$

(b)

$R_{b12} = 3.96$
$R_{b23} = 3.86$
$R_{b34} = 3.50$
$R_{b45} = 4.00$

$T_{12} = 0$ $T_{13} = 2$ $T_{14} = 4$ $T_{15} = 8$
$T_{23} = 0$ $T_{24} = 2$ $T_{25} = 4$
$T_{34} = 0$ $T_{35} = 2$
$T_{45} = 0$

(c)

Fig. 10 **(a)** Branch number matrix for the Tokunaga tree illustrated in Fig. 8. **(b)** Branch numbers and bifurcation ratios. The bifurcation ratio approaches 4 ($D \to 2$) for high orders. **(c)** Branch-ratio matrix for the tree.

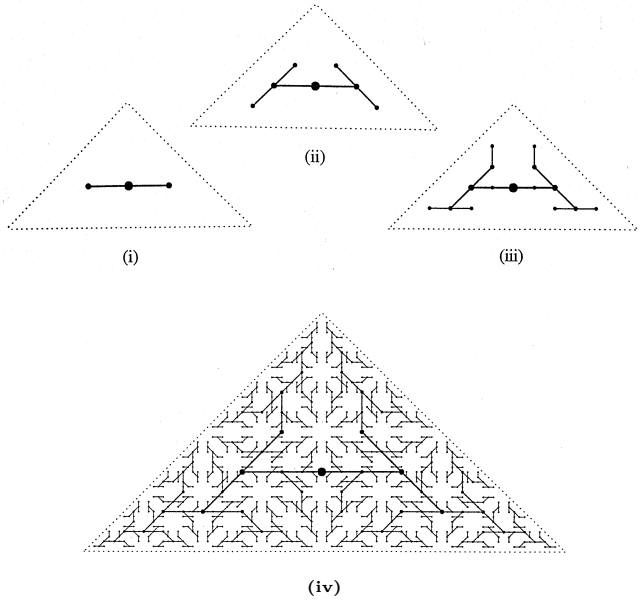

(a)

Fig. 11 Two deterministic binary fractal trees with side branching based on right triangles. With $R_r = 2^{1/2}$ the constructions are space filling without overlap. In each case, first, second, third, and ninth order examples are given.

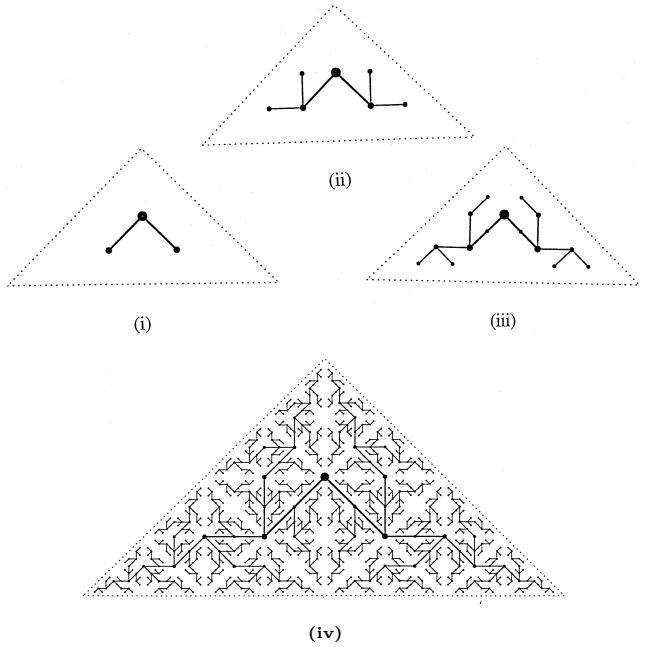

(b)

Fig. 11 (*Continued*)

Again applying Eq. (11) the appropriate matrix A is given by

$$A = \begin{pmatrix} 3 & 2 & 0 & 2 \\ 1 & 0 & 0 & 1 \\ 0 & 1 & 1 & 0 \\ 0 & 1 & 3 & 1 \end{pmatrix} . \qquad (17)$$

The eigenvalues of this matrix are $\lambda = 4, 1, 0, 0$. For large orders the eigenvalue $\lambda = 4$ again dominates which is consistent with $R_b \to 4$.

Many other constructions that asymptotically become space filling can be devised. Two examples based on right triangles are given in Fig. 13. Fifth-order and ninth-order examples of each construction are given.

Space filling fractal trees can also be constructed in three dimensions. A binary example with no side branching is illustrated in Fig. 12. For this construction we have $R_b = 2$ and $R_r = 2^{1/3}$ so that $D = 3$. When extended to infinite order this construction becomes completely volume filling without overlap. The construction illustrated in Fig. 12 is the three-dimensional analog to the two-dimensional construction illustrated in Fig. 4.

We next illustrate a deterministic volume filling fractal tree with side branching. The first three iterations are illustrated in Fig. 13. Instead of being a ternary construction with three branches attached to each tip node, this construction has seven

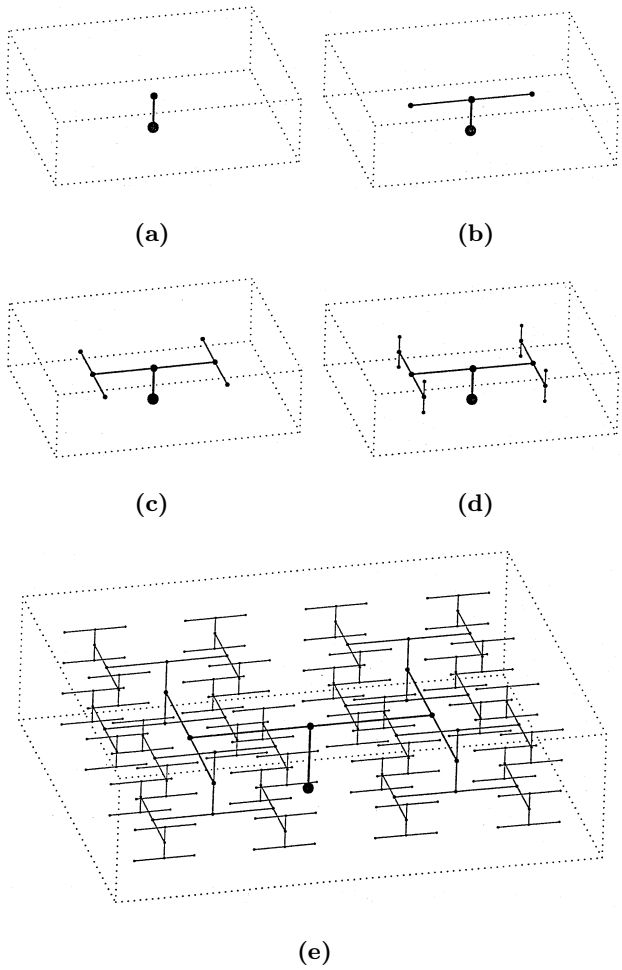

Fig. 12 Three-dimensional binary fractal tree. With $R_b = 2$ and $R_r = 2^{1/3}$ we have $D = 3$, the construction is volume filling without overlap. **(a)** First-order example. **(b)** Second-order example. **(c)** Third-order example. **(d)** Fourth-order example. **(e)** Eighth-order example.

branches attached to each tip node. This construction is based on a hierarchy of body-centered cubic lattices. We use a generator A given in Fig. 13(a). At first order a branch extends from one corner of cube to the center of the cube, with a tip node placed at its end. The unit cube at first order is divided into eight cubes with $r_2 = 1/2$ at second order. At second order branches extend from the central node to the centers of the eight cubes. Due to the overlapping with the first-order branch, one of these cubes produces a new generator B (diagonal of the cube with an internal node at the center) while the other seven cubes have no overlapping and produce seven rescaled versions of the generator A. Each of the eight cubes at second order is further divided into eight cubes with $r_3 = 1/4$ at third order. The seven second-order cubes with generator

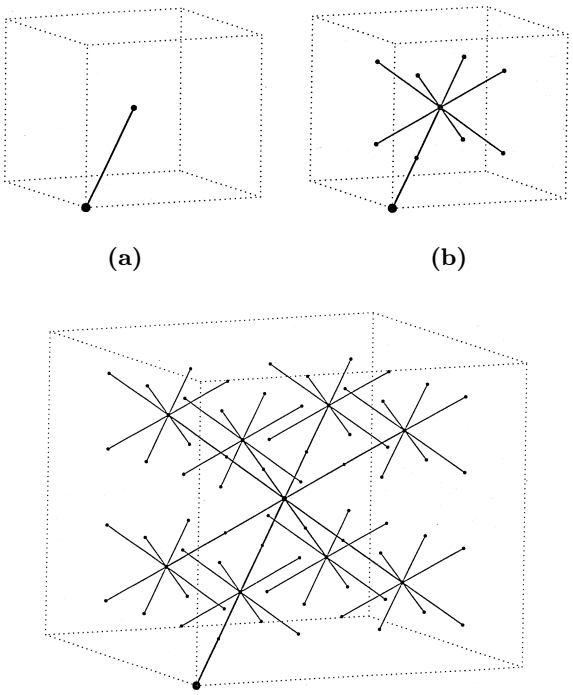

Fig. 13 Deterministic third-order, volume filling fractal tree with side branching and $R_r = 2$. The construction is based on a body-centered cubic lattice. Tip nodes emit seven branches at each order and internal nodes emit six branches.

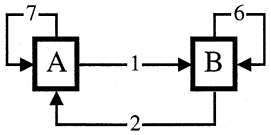

Fig. 14 Flow chart indicating how the terminal branch generator A and internal branch generator B are used to construct the volume filling fractal tree illustrated in Fig. 15.

A are treated in the exact same way at third order. The eighth second-order cube, with generator B, produces six third-order cubes with generator A, and two cubes with generator B. These steps are repeated at all higher orders. A flow chart illustrating the construction of this three dimensional fractal tree is given in Fig. 14.

The length-order ratio for this construction is $R_r = 2$. The branch-number and branch-ratio matrices for this construction are given in Fig. 15(a) and 15(c). The branching ratios for arbitrary order are given by

$$R_k = \begin{cases} 0 & \text{k=1} \\ 6 \times 2^{k-2} & \text{k= } 2, 3, 4, \ldots \end{cases} . \qquad (18)$$

$N_{11} = 3{,}073$ $N_{12} = 0$ $N_{22} = 385$ $N_{13} = 330$ $N_{23} = 0$ $N_{33} = 49$ $N_{14} = 84$ $N_{24} = 42$ $N_{34} = 0$ $N_{44} = 7$ $N_{15} = 24$ $N_{25} = 12$ $N_{35} = 6$ $N_{45} = 0$ $N_{55} = 1$

(a)

$N_1 = 3{,}511$ $N_2 = 439$ $N_3 = 55$ $N_4 = 7$ $N_5 = 1$

$R_{b12} = 8.00$ $R_{b23} = 7.98$ $R_{b34} = 7.87$ $R_{b45} = 7$

$T_{12} = 0$ $T_{13} = 6$ $T_{23} = 0$ $T_{14} = 12$ $T_{24} = 6$ $T_{34} = 0$ $T_{15} = 24$ $T_{25} = 12$ $T_{35} = 6$ $T_{45} = 0$

(b) (c)

Fig. 15 **(a)** Branch number matrix for the Tokunaga tree illustrated in Fig. 16. **(b)** Branch numbers and bifurcation ratios. The bifurcation ratio approaches 8 ($D \to 3$) for high orders. **(c)** Branch-ratio matrix for the tree.

Again the construction is a Tokunaga fractal tree. The branch numbers and bifurcation ratios are given in Fig. 15(b). For large-order trees $R_b \to 8$ so that $D \to 3$, the construction becomes volume filling.

The recursive map for this construction is

$$n_A(i+1) = 7n_A(i) + 6n_B(i) \qquad (19)$$

$$n_B(i+1) = n_A(i) + 2n_B(i) \qquad (20)$$

Again applying Eq. (11) the appropriate matrix A is given by

$$A = \begin{pmatrix} 7 & 6 \\ 1 & 2 \end{pmatrix} . \qquad (21)$$

The eigenvalues of this matrix are $\lambda = 8, 1$. For large orders the eigenvalue 8 again dominates which is consistent with $R_b \to 8$.

3. APPLICATIONS

3.1 Diffusion Limited Aggregation (DLA)

The concept of diffusion limited aggregation (DLA) was introduced by Witten and Sander.[7] They considered a grid of points on a two-dimensional lattice and placed a seed particle near the center of the grid. An accreting particle was randomly introduced on a "launching" circle and was allowed to follow a random path until: i) it accreted to the growing cluster of particles by entering a grid point adjacent to the cluster or ii) until it wandered across a larger "killing" circle. The resulting sparse,

tree-like structure has been taken as an excellent representation of dendritic growth patterns found both in nature and in industrial applications.[8]

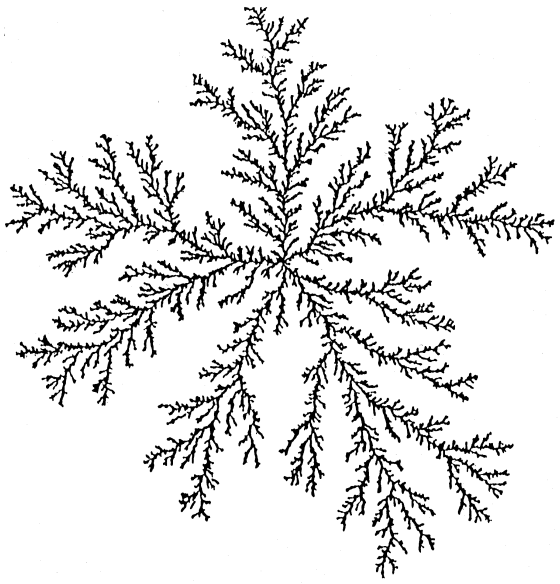

Fig. 16 A two-dimensional, off-lattice DLA cluster with 10^6 particles.[9]

Ossadnik[9] has considered the branching statistics of 47 off-lattice DLA clusters each with 10^6 particles, a typical example being illustrated in Fig. 16. On average the networks were 11th order fractal trees. The average bifurcation ratio for the clusters was found to $R_b = 5.15 \pm 0.05$ and the average length-order ratio $R_r = 2.86 \pm 0.05$, from Eq. (3) the corresponding fractal dimension is $D = 1.56$. In order to analyze the branching statistics of DLA clusters Ossadnik[9] utilized the ramification matrix introduced for DLA by Vannimenus and Viennot.[10] In terms of the branching ratios T_{ij} the terms of the ramification matrix are defined by

$$R_{ij} = \frac{T_{ij}}{\sum_{i,\ i<j} T_{ij}} . \tag{22}$$

The terms of the ramification-matrix obtained for DLA by Ossadnik[9] are given in Fig. 17. For a Tokunaga self-similar fractal tree for which Eq. (6) is valid, the terms of the ramification matrix are given by

$$R_{ij} = \frac{c^{j-i-1}}{\sum_{i,\ i<j} c_{ij}} . \tag{23}$$

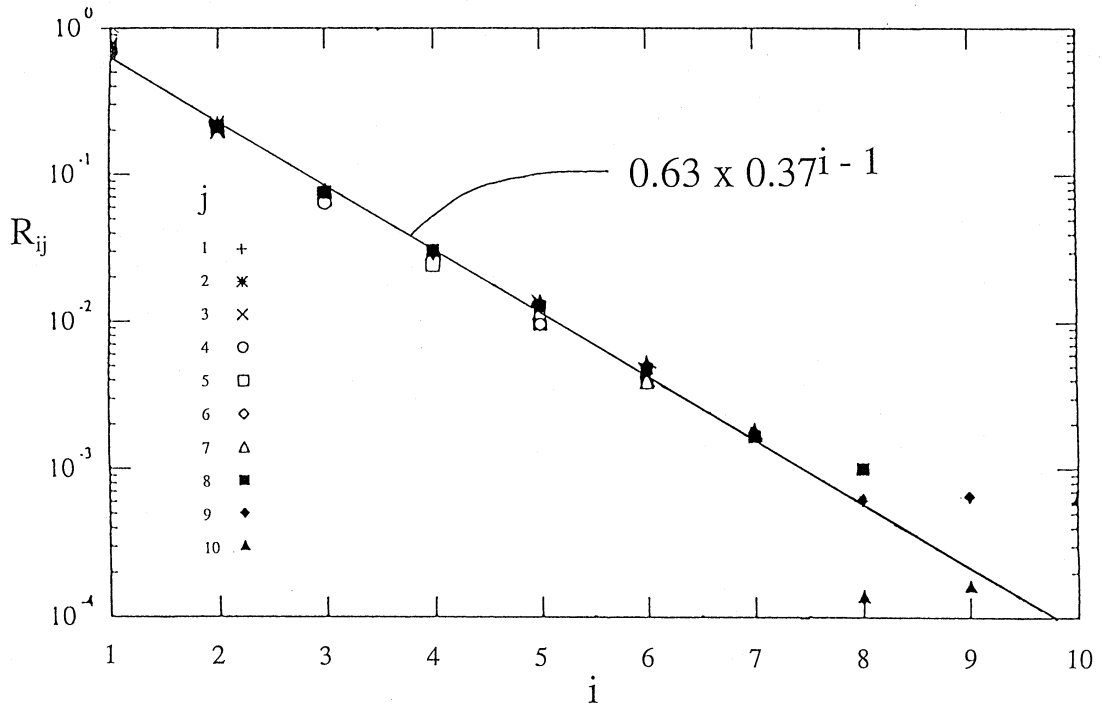

Fig. 17 Dependence of the terms of the ramification matrix R_{ij} for the branching statistics of a diffusion limited aggregation (DLA) cluster on the branch order i for various branch orders j. Branches of order i join branches of order j so that $i < j$. The data points are for an average of 47 off-lattice DLA clusters each with 10^6 particles.[9] The straight-line correlation is with the Tokunaga relation [Eq. (6)] taking $c = 2.7$.

For large values of j this becomes

$$R_{ij} = \frac{1}{c^{i-1}} \left(1 - \frac{1}{c}\right) . \tag{24}$$

Taking $c = 2.7$ this relation is compared with the DLA data given in Fig. 17. It is seen that DLA clusters are Tokunaga self-similar fractal trees to a good approximation.

3.2 River Networks

We now address the question of whether the statistics of actual drainage networks are represented by Tokunaga fractal trees. Peckham[10] has determined branching-ratio matrices for the Kentucky River basin in Kentucky and the Powder River basin Wyoming. Both are 8th order basins with the Kentucky River basin having an area of 13,500 km^2 and the Powder River basin an area of 20,181 km^2. For the Kentucky River basin the bifurcation ratio is $R_b = 4.6$ and the length-order ratio is $R_r = 2.5$; for the Powder River basin the bifurcation ratio is $R_b = 4.7$ and the length-order ratio is $R_r = 2.4$. From Eq. (3) the corresponding values of the fractal dimension are $D = 1.67$ and $D = 1.77$ respectively. The branching-ratio matrices for the two river basins are given in Fig. 18. We now determine values for T_k by averaging the values of $T_{i,i+k}$ over i

$$T_k = \frac{1}{n-k} \sum_{i=1}^{n-k} T_{i,i+k} . \tag{25}$$

The values of T_k for the two basins are given in Fig. 19 as a function of k. It is seen that the results correlate well with Eq. (6) taking $a = 1.2$ and

1.1	3.2	7.6	15.6	54.8	87.0	408.0
	1.1	2.8	6.2	20.3	27.0	115.0
		1.2	2.9	10.8	16.0	40.0
			1.0	3.2	5.3	20.0
				1.8	2.0	12.0
					1.0	3.0
						1.0

(a)

1.1	3.8	11.5	32.9	72.4	90.0	276.0
	1.2	3.4	9.8	24.3	37.0	82.0
		1.1	3.3	8.8	11.7	54.0
			1.5	3.9	6.0	25.0
				1.5	1.3	9.0
					0.7	5.0
						1.0

(b)

Fig. 18 Branching-ratio matrices for **(a)** the Kentucky River basin and **(b)** the Powder River basin as obtained by Peckham.[11]

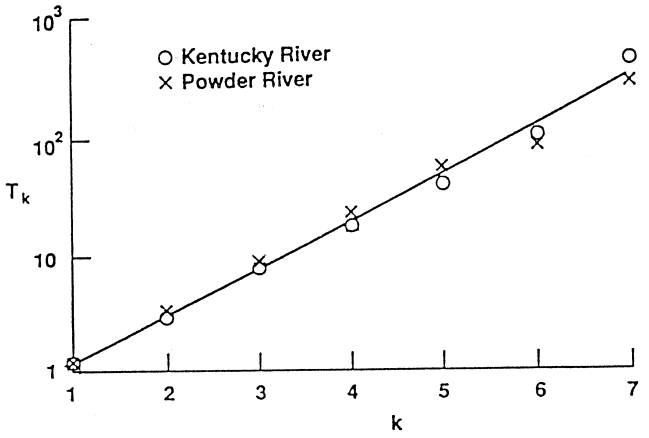

Fig. 19 Dependence of the mean branching ratios T_k on k for the Kentucky River basin and the Powder River basin. The straight-line correlation is with Eq. (6) taking $a = 1.2$ and $c = 2.5$.

$c = 2.5$. For these two basins, in quite different geological settings, good agreement with Tokunaga fractal trees is obtained with these values of the parameters a and c.

3.3 Biology

Fractal trees have had a number of applications in biology.[12,13] These include plants and trees, root systems, bronchial systems, cardiovascular systems, and the brain. Many authors have applied the Strahler ordering system with a wide variety of results. There are clearly wide opportunities to apply the Tokunaga ordering system in biology.

As a preliminary study of side branching in biology we have obtained the branching statistics for a shagbark hickory (*carya ovata*). The branch-number matrix for this sixth-order example is given in Fig. 20(a). The numbers of branches of each order along with bifurcation ratios are given in Fig. 20(b). The mean bifurcation ratio is $R_b = 3.16$. The mean lengths of the branches of the five lowest orders along with the length-order ratios are also given in Fig. 20(b). The mean length-order ratio is $R_r = 2.26$. From Eq. (3) the corresponding fractal dimension is $D = 1.41$. The three-dimensional canopy of branches is relatively sparse.

The branching-ratio matrix for the shagbark hickory is given in Fig. 20(c). Taking averages to find T_k using Eq. (22), we find $T_1 = 0.79$, $T_2 = 1.07$, $T_3 = 0.79$, $T_4 = 1.67$, and $T_5 = 3$. The scatter of the data is considerable and the applicability of the

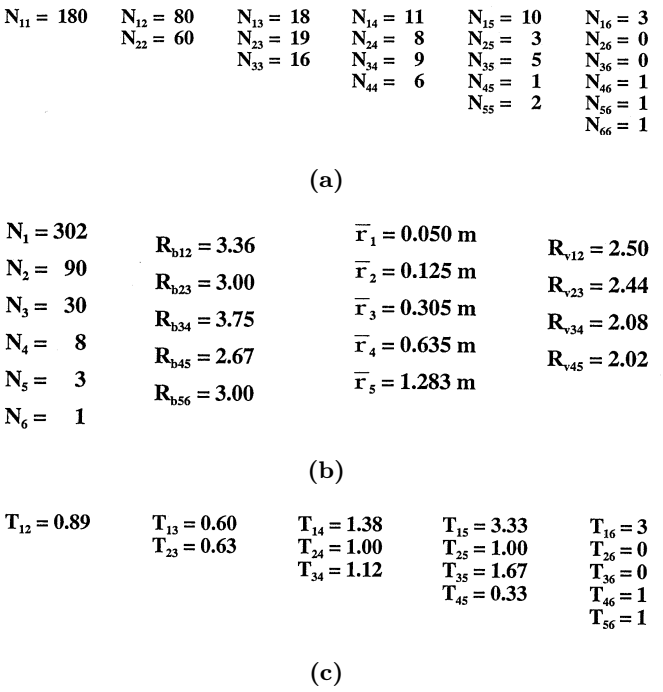

Fig. 20 **(a)** Branch-number matrix for a sixth-order shagbark hickory (*carya ovata*). **(b)** Branch-numbers, bifurcation ratios, mean lengths, and length-order ratios. **(c)** Branching-ratio matrix.

Tokunaga relation Eq. (6) can certainly be questioned. However, as an approximation we will take $a = 1$ and $c = 1$. There is relatively little side branching on the shagbark hickory. This example is not meant to be a definitive study, but rather is intended to illustrate how the Tokunaga ordering system can be applied to biological problems.

4. CONCLUSIONS

The basic purpose of this paper is to address the role of side branching in the consideration of self-similar fractal trees. The classical Strahler ordering system has been widely used to quantify hierarchical networks. Developed for drainage networks, the Strahler classification defines constant bifurcation ratios and length-order ratios for self-similar networks. The fractal dimension of these networks is defined using Eq. (3). However, a uniform feature of actual self-similar networks is side branching. Tokunaga[4,5,6] introduced a side-branching classification system for quantification of side-branching statistics. He further introduced a self-similar scaling [Eq. (6)] for the side-branching statistics. The Tokunaga classification scheme clearly provides an improved taxonomy for self-similar networks.

We have introduced deterministic constructions for space filling ($D = 2$) and volume filling ($D = 3$) trees. In each case, we have given alternative constructions with and without side branching. The examples with side branching conform with Tokunaga self-similarity [Eq. (6)] statistics.

Diffusion limited aggregation (DLA) describes a mechanism, as well as a numerical technique, for generating self-similar networks. The side-branching statistics of DLA clusters obey the Tokunaga relation [Eq. (6)]. The side-branching statistics of actual drainage networks have also been shown to satisfy the Tokunaga relation [Eq. (6)]. A wide variety of models have been developed for drainage networks. In general, these models give fractal statistics that are in reasonable agreement with observations. However, the requirement that models also produce the appropriate Tokunaga statistics is a more robust requirement. Masek and Turcotte[14] proposed a model for headward migration of drainage networks based on DLA. This model yields Tokunaga statistics which are in good agreement with the results obtained by Peckham.[10]

One of the most promising areas for the future application of the Tokunaga taxonomy is in biology. Branching statistics are applicable to plants and trees, root systems, bronchial systems, cardiovascular systems, and the brain. All of these biological applications clearly include extensive side branching. The use of nodes (buds) to generate growing networks with both tip and side branches strongly resembles many growth processes in nature. Other possible future applications include evolutionary trees, the nervous system, and computer networking.

ACKNOWLEDGMENTS

This work was partially supported (DLT) by NASA Grant NAGW-4702.

REFERENCES

1. B. Mandelbrot, "How Long is the Coast of Britain? Statistical Self-Similarity and Fractional Dimension," *Science* **156**, 636 (1967).
2. R. E. Horton, "Erosional Development of Streams and their Drainage Basins; Hydrophysical Approach to Quantitative Morphology," *Geol. Soc. Am. Bull.* **56**, 275 (1945).

3. A. N. Strahler, "Quantitative Analysis of Watershed Geomorphology," *Am. Geophys. Un. Trans.* **38**, 913 (1957).
4. E. Tokunaga, "Consideration on the Composition of Drainage Networks and their Evolution," *Geographical Rep. Tokyo Metro. Univ.* **13**, 1 (1978).
5. E. Tokunaga, "Ordering of Divide Segments and Law of Divide Segment Numbers," *Jap. Geomorph. Un.* **5**, 71 (1984).
6. E. Tokunaga, "Selfsimilar Natures of Drainage Basins," in *Research of Pattern Formation*, ed. R. Takaki, (KTK Scientific Publishers, Tokyo, 1994), p. 445.
7. T. A. Witten and L. M. Sander, "Diffusion-Limited Aggregation, a Kinetic Critical Phenomenon," *Phys. Rev. Let.* **47**, 1400 (1981).
8. A. D. Fowler, "Self-Organized Mineral Textures of Igneous Rocks: The Fractal Approach," *Earth-Sci. Rev.* **29**, 47 (1990).
9. P. Ossadnik, "Branch Order and Ramification Analysis of Large Diffusion Limited Aggregation Clusters," *Phys. Rev.* **A45**, 1058 (1992).
10. J. Vannimenus and X. G. Viennot, "Combinatorial Tool for the Analysis of Ramified Patterns," *J. Stat. Phys.* **54**, 1529 (1989).
11. S. D. Peckham, "New Results for Self-Similar Trees with Applications to River Networks," *Water Resour. Res.* **31**, 1023 (1989).
12. N. MacDonald, *Trees and Networks in Biological Models* (John Wiley and Sons, Chichester, 1983).
13. J. B. Bassingthwaighte, L. S. Liegovitch, and B. J. West, *Fractal Physiology* (Oxford University Press, 1994).
14. J. G. Masek and D. L. Turcotte, "A Diffusion Limited Aggregation Model for the Evolution of Drainage Networks," *Earth Planet. Sci. Let.* **119**, 379 (1993).